

A study of carbon substitutions in MgB_2 within the two-band Eliashberg theory

G.A. Ummarino,* D. Daghero, and R.S. Gonnelli

*Dipartimento di Fisica, Politecnico di Torino, Corso Duca degli Abruzzi 24, 10129 Torino, Italy and
INFN- LAMIA, Corso Perrone 24, 16152 Genova, Italy*

A.H. Moudden

Laboratoire Léon Brillouin, CEA-CNRS, CE Saclay, 91191 Gif-sur-Yvette, France

We study the effects of C substitutions in MgB_2 within the two-band model in the Eliashberg formulation. We use as input the $B-B$ stretching-mode frequency and the partial densities of states $N_N^\sigma(E_F)$ and $N_N^\pi(E_F)$, recently calculated for $\text{Mg}(\text{B}_{1-x}\text{C}_x)_2$ at various x values from first-principles density functional methods. We then take the prefactor in the Coulomb pseudopotential matrix, μ , and the interband scattering parameter, $\Gamma^{\sigma\pi}$, as the only adjustable parameters. The dependence on the C content of T_c and of the gaps (Δ_σ and Δ_π) recently measured in $\text{Mg}(\text{B}_{1-x}\text{C}_x)_2$ single crystals indicate an almost linear decrease of μ on increasing x , with an increase in *interband* scattering that makes the gaps merge at $x = 0.132$. In polycrystals, instead, where the gap merging is not observed, no interband scattering is required to fit the experimental data.

PACS numbers: 74.45.+c, 74.70.Ad, 74.20.Fg

In spite of its simple structure, the intermetallic compound MgB_2 – discovered to be superconducting at about 40 K in 2001 [1] – soon revealed a number of surprising features that could not be explained within a picture of conventional superconductivity. Bandstructure calculations [2] showed that the energy bands of MgB_2 can be grouped into two sets: the quasi-2D σ bands, and the 3D π bands, originating from the superposition of in-plane and out-of-plane boron orbitals, respectively. As a matter of fact, most of the physical properties of this superconductor have found a clear and relatively simple explanation within an *effective* two-band model [3, 4, 5] in which the two bands interact via a phonon-mediated *interband coupling*. The result is that superconductivity develops in both bands at the same T_c , but with energy gaps of different amplitude, Δ_σ and Δ_π , and thus different values of the gap ratio $2\Delta/k_B T_c$. The success of the two-band model in describing the features of MgB_2 naturally opens the question whether it can predict (or at least explain a posteriori) the effects of induced disorder, irradiation and, over all, chemical substitutions on the physical properties of the compound. As far as substitutions are concerned, the experimental test of theoretical predictions has been delayed or even prevented by the technical difficulties in obtaining good-quality samples of partially substituted MgB_2 [6]. Recently, point-contact measurements of the gap amplitudes as a function of the C content have been reported in state-of-the-art $\text{Mg}(\text{B}_{1-x}\text{C}_x)_2$ polycrystals [7] and single crystals [8]. The availability of these results (that for some aspects contrast with each other) gives a good opportunity to test the two-band model. In this paper we will show that both the experimental data concerning T_c and the gaps as a function of x can be well explained within the

two-band model in the Eliashberg formulation. We will use as input the frequencies of the B-B stretching mode (which is strongly coupled to the holes in the σ band) and the partial densities of states at the Fermi level, $N_N^\sigma(E_F)$ and $N_N^\pi(E_F)$, calculated from first-principle density functional methods adopting the viewpoint of ordered supercells [9] instead of the virtual-crystal approximation. Then, we will show that the experimental x dependence of T_c and of the gaps Δ_σ and Δ_π can be very well reproduced by admitting a reasonable x dependence of the prefactor in the Coulomb pseudopotential matrix [4, 10] and, in the case of single crystals, an increase in the *interband scattering* $\Gamma^{\sigma\pi}$ on increasing the C content.

Let us start from the generalization of the Eliashberg theory [11, 12] for systems with two bands [13], that has already been used with success to study the MgB_2 system [4, 5, 10, 14, 15, 16]. To obtain the gaps and the critical temperature within the s -wave, two-band Eliashberg model one has to solve four coupled integral equations for the gaps $\Delta_i(i\omega_n)$ and the renormalization functions $Z_i(i\omega_n)$, where i is a band index and ω_n are the Matsubara frequencies. We included in the equations (explicitly reported elsewhere [14]) the non-magnetic impurity scattering rates in the Born approximation, Γ^{ij} .

The solution of the Eliashberg equations requires as input: i) the four (but only three independent[13]) electron-phonon spectral functions $\alpha_{ij}^2(\omega)F(\omega)$; ii) the four (but only three independent[13]) elements of the Coulomb pseudopotential matrix $\mu^*(\omega_c)$; iii) the two (but only one independent [13]) effective impurity scattering rates Γ^{ij} . None of these parameters or functions has been calculated for C-substituted MgB_2 , and in many cases their determination is a very difficult task, at least at the present moment. Hence, we are left with a problem with too many degrees of freedom. However, we will now show how some reasonable approximations allow reducing the number of adjustable parameters to 2, with no significant loss of generality.

*Electronic address: E-mail:giovanni.ummarino@infm.polito.it

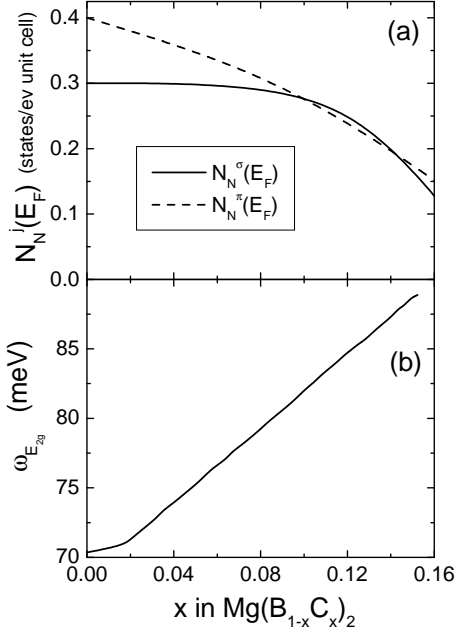


FIG. 1: (a) Calculated density of states at the Fermi energy, $N_N^\sigma(E_F)$ (solid line) and $N_N^\pi(E_F)$ (dashed line) as a function of x (From Ref. 9). (b) Calculated frequency of the B-B bond stretching mode (the E_{2g} mode in pure MgB_2) as a function of x (from Ref. 9).

Let's start with the four spectral functions $\alpha_{ij}^2(\omega)F(\omega)$, that were calculated for pure MgB_2 in ref. 10. For simplicity, we will assume that the shape of the $\alpha_{ij}^2F(\omega, x)$ functions does not change with x , and we will only rescale them with the electron-phonon coupling constants λ_{ij} :

$$\alpha_{ij}^2F(\omega, x) = \frac{\lambda_{ij}(x)}{\lambda_{ij}(x=0)} \alpha_{ij}^2F(\omega, x=0) \quad (1)$$

Neglecting the effect of C substitution on the shape of the e-ph spectral functions is not a dramatic simplification, since we showed in a previous paper [14] that the details of $\alpha^2F(\omega)$ do not significantly affect the resulting T_c . To determine the scaling factor in eq. 1, let us remind that, from the definition of electron-phonon coupling constant [17]:

$$\lambda = \frac{N_N(E_F) \langle I^2 \rangle}{M\Omega_0^2} \quad (2)$$

where M is the ion mass, Ω_0 is a frequency representative of the phonon spectrum, $N_N(E_F)$ is the density of states at the Fermi level and $\langle I^2 \rangle$ is the average matrix element of the electron-ion interaction [17]. In our case, M is the boron mass [3] and does not depend on x . As a first approximation, and as we did in the case of Al substitution [14], we will assume that also the average matrix element of the electron-ion interaction $\langle I^2 \rangle$ is constant, because it is basically determined by the deformation potential which is almost independent of x [18].

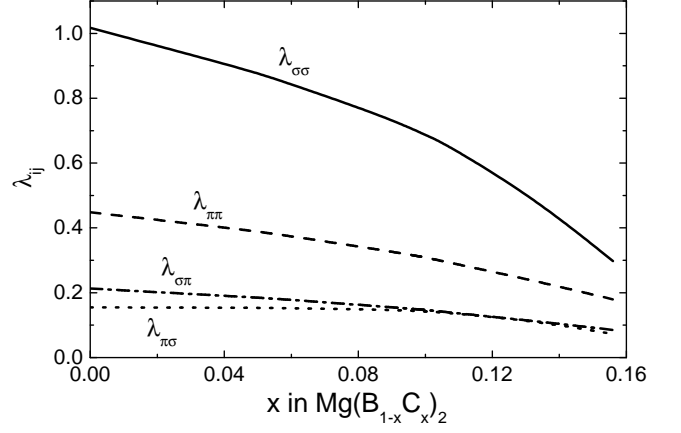


FIG. 2: Electron-phonon coupling constants λ_{ij} calculated as a function of x according to eqs. 3 and 4.

The partial densities of states at the Fermi level, $N_N^\sigma(E_F)$ and $N_N^\pi(E_F)$, have been recently calculated from first principles by using a supercell approach [9] for different values of the C content x , and are reported in Fig.1(a). The frequency Ω_0 can be identified with the frequency of the B-B bond-stretching phonon mode (the E_{2g} mode), that has been recently calculated as a function of x from first principles [9], and is reported in Fig.1(b). Since this mode couples strongly with the holes on top of the σ band, from eq. 2 we will have for $\lambda_{\sigma\sigma}$ (which gives the most important contribution to superconductivity in our system):

$$\lambda_{\sigma\sigma}(x) = \frac{N_N^\sigma(E_F, x)\omega_{E_{2g}}^2(x=0)}{N_N^\sigma(E_F, x=0)\omega_{E_{2g}}^2(x)} \lambda_{\sigma\sigma}(x=0). \quad (3)$$

In this way, we assume that the change in the frequency of the E_{2g} phonon affects the coupling constant, while we neglect its influence on the shape of the electron-phonon spectral function. For the other coupling constants, we will instead assume for simplicity

$$\forall(i, j) \neq (\sigma, \sigma) \quad \lambda_{ij}(x) = \frac{N_N^j(E_F, x)}{N_N^j(E_F, x=0)} \lambda_{ij}(x=0) \quad (4)$$

with $\lambda_{\sigma\sigma}(x=0)=1.017$, $\lambda_{\pi\pi}(x=0)=0.448$, $\lambda_{\sigma\pi}(x=0)=0.213$ and $\lambda_{\pi\sigma}(x=0)=0.155$ [4, 10]. Fig. 2 shows the calculated electron-phonon coupling constants λ_{ij} as a function of x .

As far as the Coulomb pseudopotential is concerned, let us start from its expression in pure MgB_2 [4, 10, 19]:

$$\begin{aligned} \mu^*(x) &= \begin{vmatrix} \mu_{\sigma\sigma}^* & \mu_{\sigma\pi}^* \\ \mu_{\pi\sigma}^* & \mu_{\pi\pi}^* \end{vmatrix} = \\ &= \mu(\omega_c, x) N_N^{\text{tot}}(E_F, x) \begin{vmatrix} \frac{2.23}{N_N^\sigma(E_F, x)} & \frac{1}{N_N^\sigma(E_F, x)} \\ \frac{1}{N_N^\pi(E_F, x)} & \frac{2.48}{N_N^\pi(E_F, x)} \end{vmatrix} \end{aligned} \quad (5)$$

where $\mu(\omega_c, x)$ is a free parameter and $N_N^{\text{tot}}(E_F, x)$ is the total normal density of states at the Fermi level. The

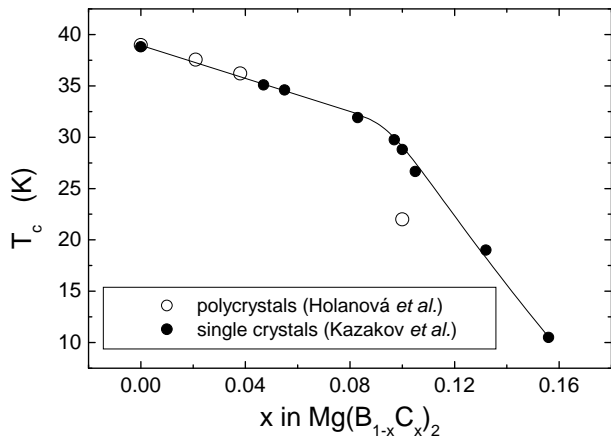


FIG. 3: The experimental T_c measured in $\text{Mg}(\text{B}_{1-x}\text{C}_x)_2$ single crystals [21] (solid circles) and polycrystals [7] (open circles) as a function of x . The line is only a guide to the eye.

numbers 2.23 and 2.48 in the Coulomb matrix have been calculated for pure MgB_2 but, as a first approximation, we will suppose them not to depend on x . In this way, the elements of the Coulomb pseudopotential matrix, μ_{ij}^* , depend on x only through the densities of states at the Fermi level and through the common prefactor $\mu(\omega_c, x)$, that could also take into account the effects of disorder.

As far as the scattering rates are concerned, let us remind that, due to Anderson's theorem, *intra*band scattering does not affect neither T_c nor the gaps [20], so we will disregard both $\Gamma^{\sigma\sigma}$ and $\Gamma^{\pi\pi}$. The remaining interband scattering parameters are related to each other since [13]

$$\frac{\lambda_{ij}(x)}{\lambda_{ji}(x)} = \frac{\mu_{ij}^*(x)}{\mu_{ji}^*(x)} = \frac{\Gamma^{ij}(x)}{\Gamma^{ji}(x)} = \frac{N_N^j(E_F, x)}{N_N^i(E_F, x)} \quad (6)$$

and thus we will always refer only to $\Gamma^{\sigma\pi}$. Finally, we can fix the cut-off energy (e.g., $\omega_c = 700$ meV) so as to reduce the number of adjustable parameters to two: the prefactor in the Coulomb pseudopotential, $\mu(\omega_c)$ (that we will call simply μ from now on) and the interband scattering parameter $\Gamma^{\sigma\pi}$.

As already pointed out, the aim of the present work is to show that the experimental dependence of T_c and of the gaps, Δ_σ and Δ_π , on the C content in $\text{Mg}(\text{B}_{1-x}\text{C}_x)_2$ can be explained within the two-band Eliashberg theory. The experimental $T_c(x)$ curves measured in single crystals [21] and polycrystals [7] are reported in Fig.3. The corresponding x dependencies of the gaps measured by point-contact spectroscopy (PCS) are reported in Fig. 4 and Fig. 8, respectively (symbols). In single crystals (Fig. 4), the two gaps approach each other on increasing x , until at $x = 0.132$ they become experimentally indistinguishable. This means that, at this doping content, their amplitudes are equal to each other within the experimental uncertainty. In polycrystals, instead, the two gaps remain clearly distinct up to $x = 0.10$, where Δ_π is much smaller than in single crystals with the same C content (see Fig. 8).

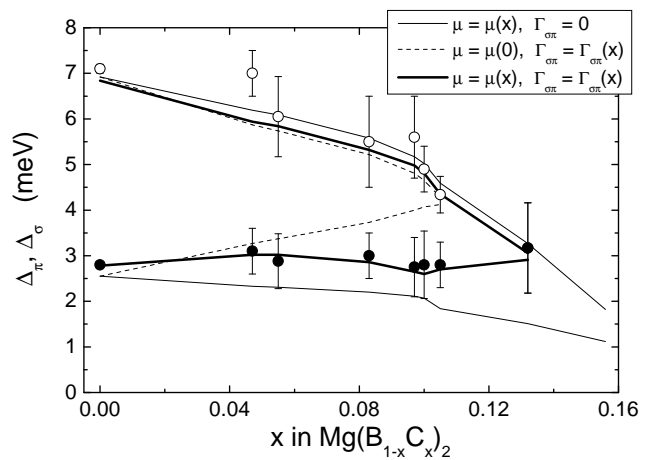


FIG. 4: Symbols: experimental values of Δ_σ (open circles) and Δ_π (solid circles) measured at $T = 4.2$ K by PCS in single crystals (from Ref. 8). Lines: Δ_i ($i\omega_n=0$) calculated for the σ and π bands at $T = T_c/4$ by solving the imaginary-axis Eliashberg equations in the following cases: i) thin solid line: $\Gamma^{\sigma\pi}=0$, and μ varies with x as shown in Fig. 5(a), open circles; ii) dashed line: $\mu(x) = \mu(0)$ and $\Gamma^{\sigma\pi}$ varies with x as shown in Fig. 5(b), open squares; iii) thick solid line: both μ and $\Gamma^{\sigma\pi}$ vary with x as shown in Fig. 5(a) and (b), respectively (solid symbols).

Let us focus for the time being on single crystals. The $T_c(x)$ curve (solid circles in Fig. 3) can be exactly reproduced by adjusting only one of the two free parameters of the model, or both of them at the same time (but, in this case, the choice of their values is not univocal unless one adds another constraint).

For example, one can keep μ equal to its value in pure MgB_2 (i.e., $\mu(x) = \mu(0)$), and view the substituted compound as a “disordered” version of MgB_2 , as if the only effect of C substitution was an increase in interband scattering. This implies neglecting also the phonon hardening and the electron-doping effects (that actually play a leading role in determining the observed $T_c(x)$ curve [22]) so that the $T_c(x)$ curve is reproduced by only varying $\Gamma^{\sigma\pi}$. The resulting trend of the interband scattering rate is shown in Fig.5(a) (open squares). Notice that with this approach one cannot obtain critical temperatures lower than $T_c = 25.8$ K, that corresponds to the isotropic “dirty” limit in which the two gaps merge into one of amplitude $\Delta = 4.1$ meV [3]. This is clearly seen in the x dependence of the gaps calculated with these values of $\Gamma^{\sigma\pi}$, which is reported in Fig. 4 as a dashed line. In spite of a rather good agreement between experimental and theoretical values of Δ_σ , the model predicts an increase in Δ_π which is not observed, and the merging of the two gaps at a much lower C content with respect to the actual one.

The opposite case consists in taking into account all the effects of substitutions (i.e. phonon hardening and electron doping), with no increase of interband scattering. In this case, one can keep $\Gamma^{\sigma\pi} = 0$, and vary μ

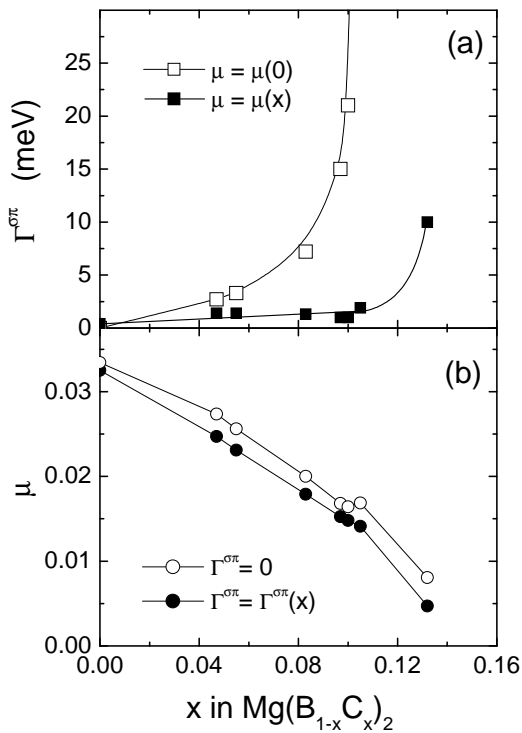


FIG. 5: (a) Open squares: the x dependence of $\Gamma^{\sigma\pi}$ necessary to reproduce the T_c of single crystals, if $\mu(x) = \mu(0)$. Solid squares: the $\Gamma^{\sigma\pi}(x)$ curve that allows fitting both T_c and the gaps when also μ is varied with x . Lines are only guides to the eye. (b) Open circles: the x dependence of the prefactor in the Coulomb pseudopotential, μ , that gives the $T_c(x)$ curve measured in single crystals (solid symbols in Fig.3), when $\Gamma^{\sigma\pi} = 0$. Solid circles: the $\mu(x)$ curve that allows fitting both T_c and the gaps (Δ_σ and Δ_π) in single crystals, when also $\Gamma^{\sigma\pi}$ is varied.

with x so as to reproduce the experimental $T_c(x)$ curve. With the resulting values of $\mu(x)$, shown in Fig.5(b) as open circles, one obtains the x dependence of the gaps indicated in Fig. 4 as thin solid lines. It is clear that the $\mu(x)$ curve that reproduces the experimental T_c for any C content gives values of the large gap Δ_σ that agree rather well with the experimental ones (open circles in Fig. 4) but gives rise to a decrease in the small gap which is not observed experimentally.

The analysis of the previous two cases suggests that the experimental $\Delta_\sigma(x)$ and $\Delta_\pi(x)$ curves could be explained as due to the interplay between a decrease in μ (that makes Δ_π decrease) and an increase in $\Gamma^{\sigma\pi}$ (that instead makes Δ_π increase). This result has been recently anticipated by an analysis of the effects of band filling and interband scattering [22]. Hence, we will now try to fit the experimental x dependence of T_c and of the gaps Δ_π and Δ_σ by varying *both* μ and $\Gamma^{\sigma\pi}$. The best-fitting curves for the gaps (actually, the values of $\Delta(i\omega_{n=0})$ at $T = T_c/4$, for the two bands) are reported as thick solid lines in Fig. 4. The choice of the parameters is univocal, and the resulting x dependencies of $\Gamma^{\sigma\pi}$

and μ are reported as solid symbols in Fig. 5(a) and (b), respectively.

As shown in Fig. 5(a), the interband scattering remains smaller than 2 meV (which is a value reasonable even for pure MgB_2) up to $x = 0.10$ and then increases to make the gaps approach each other until they become indistinguishable. The point at $x = 0.132$ in Fig. 5(a) represents the minimum value of $\Gamma^{\sigma\pi}$ that gives gap values differing less than 0.3 meV (which is approximately the best experimental resolution of PCS at 4.2 K). Greater values of $\Gamma^{\sigma\pi}$ are allowed as well, since they would give rise to gaps even closer to each other. Although the point at $x = 0.132$ might depend on the approximations we are using in the present paper, there is no doubt that $\Gamma^{\sigma\pi}$ has to increase to reproduce the experimental gap values [22]. This increase is thus a general prediction of the two-band Eliashberg theory, but its origin in C-substituted MgB_2 is still debated at the moment. According to Ref. 23, carbon substitutions should not change the local lattice point symmetry and therefore the interband scattering should remain very small as in pure MgB_2 [20]. However, a σ - π hybridization might also arise, above $x = 0.10$, from the presence of superstructures or even short-range order in the substituted compound [9]. It must be said, however, that high-resolution TEM has shown no superstructures in these single crystals [21], even if the possibility of short-range order is not ruled out. An alternative explanation is based on the observed increase in flux pinning and in the normalized resistance on increasing x [21]. These effects suggest the existence of microscopic defects in the single crystals, acting as scattering centers. As indicated by magnetization data, these defects might be local inhomogeneities in the C distribution on a length scale comparable to ξ , that may well give rise also to $\sigma - \pi$ scattering.

The values of the Coulomb pseudopotential prefactor, μ , that allow reproducing both the T_c and the gap amplitudes, are reported in Fig. 5(b) (solid circles) as a function of x . The resulting $\mu(x)$ curve is almost linear up to $x = 0.10$, where a change in slope reflects the analogous feature of the experimental T_c (see Fig. 3). Fig. 6 reports the values of the components of the Coulomb pseudopotential matrix, μ_{ij}^* , calculated from eq. 5 by using the densities of states ($N_N^\sigma(E_F, x)$ and $N_N^\pi(E_F, x)$) from density-functional methods, and the values of $\mu(x)$ that allow best-fitting the experimental gaps (solid symbols in Fig. 5(b)). It is clear that all the components of the μ^* matrix monotonically decrease on increasing the C content. The large decrease (by a factor of two) of μ or, similarly, of $\mu_{\sigma\sigma}^*$ between $x=0$ and $x=0.1$, suggests large changes in the electronic screening, that seem to be incompatible with the much smaller changes in the partial densities of states (Fig.1). Giving an explanation of this puzzle within the two-band model is a very difficult task. However, a tentative and qualitative explanation can be given in the much simpler single-band case. Let us therefore consider the σ -band quantities alone. Let $\mu^* \equiv \mu_{\sigma\sigma}^*$ be the renormalized Coulomb pseudopotential, given by

$\mu^* = \mu[1 + \mu \ln(E_F/\omega_{\text{log}})]^{-1}$. Starting from the value $\mu^*(x=0) \simeq 0.17$ (see Fig.6) and using $E_F=500$ meV [24] and $\omega_{\text{log}}=\omega_{E2g}$, the value of the bare Coulomb pseudopotential $\mu = 0.26$ is obtained. From the Morel-Anderson definition [25] of μ , i.e.:

$$\mu = \frac{1}{2\left(\frac{2k_F}{k_S}\right)^2} \cdot \ln \left[1 + \left(\frac{2k_F}{k_S} \right)^2 \right] \quad (7)$$

where k_S is the screening wavevector, and using as a first approximation the free-electron relationship between k_F and E_F , one gets $k_S(x=0)=0.47 \text{ \AA}^{-1}$. The same calculation gives, for $x = 0.1$, $k_S(x=0.1)=0.16 \text{ \AA}^{-1}$, so that $[(k_S(x=0)/k_S(x=0.1))]^2 = 8.56$. Since in the Morel-Anderson model $k_S^2 \propto k_{TF}^2$ (where k_{TF} is the Thomas-Fermi screening wavevector) and k_{TF}^2 is proportional to $N(E_F)$, this value has to be compared to the ratio $N_N^\sigma(E_F, x=0)/N_N^\sigma(E_F, x=0.1)=1.11$. The comparison confirms that the change in the DOS alone cannot explain the observed reduction in μ^* . However, a large increase in the residual resistivity is observed on increasing the C content [21], so that $\rho_0(x=0.1) \approx 5\rho_0(x=0)$. This suggests that, for some $x > 0.1$, a metal-to-insulator (MIT) transition might be expected. In the hypothesis that at $x = 0.1$ the system already lies somewhere between the Fermi liquid and the critical regime where the MIT occurs, a generalization of the Morel-Anderson model [26] has to be used to describe the $x = 0.1$ case. Within this scenario, $k_S^2(x=0.1) \propto k_{TF}^2[1 + (a/\alpha r)^2]^{-1}$, where $r = [\rho_0(x=0.1) - \rho_c]/\rho_c$, ρ_c is the critical value of the residual resistivity and a , α are constants defined in Ref. 26. Hence one gets

$$\left[\frac{k_S(x=0)}{k_S(x=0.1)} \right]^2 = \frac{N_N^\sigma(x=0)}{N_N^\sigma(x=0.1)} \cdot \left[1 + \left(\frac{a}{\alpha r} \right)^2 \right] \quad (8)$$

from which $(a/\alpha r) = 2.78$. The parameter αr expresses the distance from criticality (i.e. from the MIT) and can be obtained from $N_N^\sigma(E_F, x=0.1) = N_N^\sigma(E_F, x=0)[1 - \exp(-\alpha r)]$, that gives $\alpha r = 2.3$. According to Ref. 26, this value is perfectly compatible with a strongly disordered Fermi liquid. Finally, the value of the constant a turns out to be $a = 6.4$ that falls in the range of values allowed in Ref.26 and is correctly of the order of the cell parameter. In conclusion, the observed drop of $\mu_{\sigma\sigma}^*$ is due to a change in the screening length that, in turns, can be justified by the transition to a disordered Fermi liquid on increasing the C content. Incidentally, this result might further justify the observed increase in interband scattering $\Gamma^{\sigma\pi}$ at high doping levels.

At this point, all the parameters entering the two-band model in Eliashberg formulation have been determined as a function of the C content, so that in principle any relevant physical property of the superconducting state of $\text{Mg}(\text{B}_{1-x}\text{C}_x)_2$ single crystals can be calculated. For the time being, we can calculate the temperature dependence of the gaps at different C contents, that can

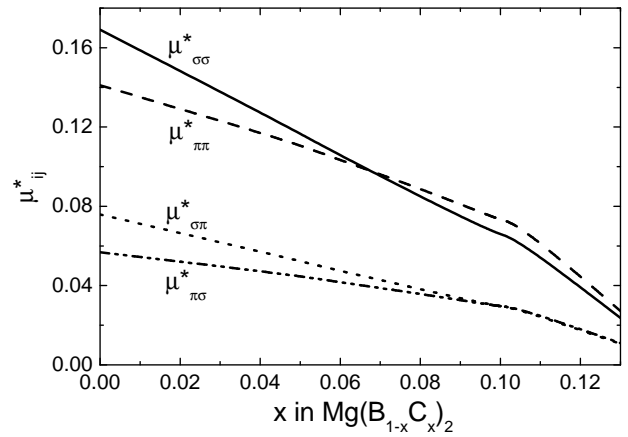


FIG. 6: The elements of the Coulomb pseudopotential matrix, μ_{ij}^* , calculated from eq.5 by using the densities of states from first-principles calculations and the prefactor $\mu(x)$ that best fits the experimental data (T_c and gaps) in $\text{Mg}(\text{B}_{1-x}\text{C}_x)_2$ single crystals.

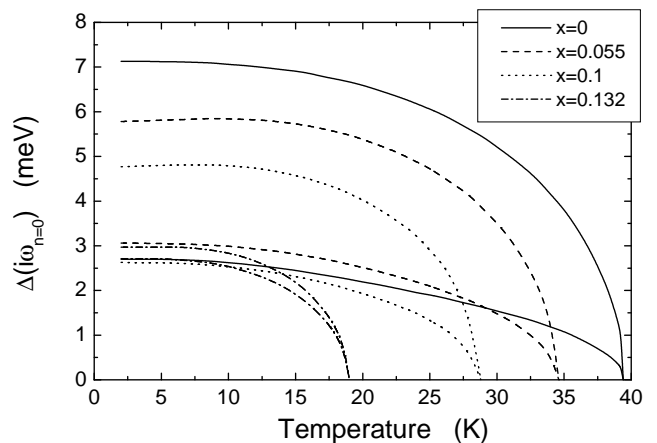


FIG. 7: The temperature dependence of $\Delta_\pi(i\omega_{n=0})$ and $\Delta_\sigma(i\omega_{n=0})$ calculated by solving the Eliashberg equations in four different cases: $x = 0$ (solid lines), $x = 0.055$ (dashed lines), $x = 0.1$ (dotted lines) and $x = 0.132$ (dash-dotted lines).

be easily tested by performing PCS measurements as a function of temperature. Fig. 7 reports the calculated values of $\Delta_\pi(i\omega_{n=0})$ and $\Delta_\sigma(i\omega_{n=0})$ as a function of T given by the solution of the Eliashberg equations in four different cases: $x = 0$ (solid lines), $x = 0.055$ (dashed lines), $x = 0.1$ (dotted lines) and $x = 0.132$ (dash-dotted lines). It is worthwhile to notice that, even at high C contents, the $\Delta_\pi(T)$ curve shows a negative curvature in the whole temperature range as in pure MgB_2 . This is due to the fact that, as shown in Fig. 2, the interband coupling does not decrease sensibly on increasing x – otherwise a positive curvature would be observed in $\Delta_\pi(T)$ in the proximity of T_c [27].

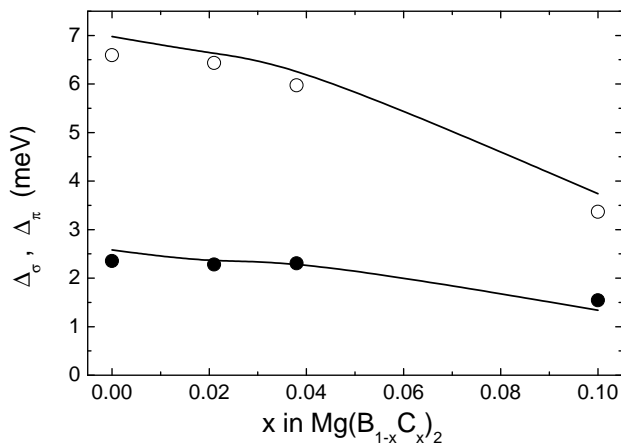


FIG. 8: Experimental values of Δ_σ (open circles) and Δ_π (solid circles) measured by PCS at $T = 4.2$ K (from Ref. 7) compared to the values of $\Delta_i(i\omega_{n=0})$ of the σ and π bands (lines) calculated by solving the imaginary-axis Eliashberg equations at $T = T_c/4$, when all the physical parameters vary with x apart from the interband scattering which is kept equal to zero.

Let us now turn our attention to the experimental results obtained in $\text{Mg}(\text{B}_{1-x}\text{C}_x)_2$ polycrystals [7]. As we did in the case of single crystals, we start by trying to reproduce the experimental $T_c(x)$ curve (open circles in Fig. 3) keeping $\Gamma^{\sigma\pi} = 0$ and varying the prefactor in the Coulomb pseudopotential, μ . Once determined the values of μ that give exactly the experimental T_c , we can calculate the gaps $\Delta(i\omega_{n=0})$ at $T = T_c/4$ for the σ and π bands. The results are reported as a function of x in Fig. 8 (solid lines). Surprisingly, the calculated gaps agree very well with those measured by PCS (symbols), with no need of interband scattering. This result indicates that the strong difference between the trend of the gaps measured in single crystals [8] and polycrystals [7] is very likely to be due to the different nature of the samples. Unfortunately, a more detailed discussion would require a deeper knowledge of the mechanisms that give rise to interband scattering in C-substituted samples, which is lacking at the present moment - even though some hypotheses for the increase in $\Gamma^{\sigma\pi}$ in single crystals have

been presented above.

In conclusion, we have studied the $\text{Mg}(\text{B}_{1-x}\text{C}_x)_2$ system within the effective two-band Eliashberg model, that was already shown to be well suited for the description of unsubstituted MgB_2 . In the analysis of the C-substituted system, we have used as input parameters the frequency of the B-B stretching mode and the partial densities of state at the Fermi level, calculated as a function of x by first-principles density-functional methods. Adopting some reasonable approximations, we have come to a simplified model with only two adjustable parameters (the prefactor in the Coulomb pseudopotential and the interband scattering rate), whose dependence on x has been determined so as to reproduce the experimental values of T_c and of the gaps Δ_σ and Δ_π .

The success of the model in describing the experimental findings shows that C-substituted MgB_2 is a weak-coupling two-band system as the parent compound. In details, the results indicate that: i) the experimental behaviour of T_c on increasing x is the results of the decrease in the $\sigma - \sigma$ intraband coupling (due to the filling of the σ bands) and of a decrease in all the elements of the Coulomb pseudopotential matrix, in particular $\mu_{\sigma\sigma}^*$. Without the contribution from μ^* , the $T_c(x)$ curve would be steeper than experimentally observed [22]; ii) the different trend of the gaps observed experimentally in single crystals (where the gaps become indistinguishable at $x = 0.132$) and polycrystals (where there is no tendency to gap merging) only arises from the different amount of interband scattering in the two cases. The increase in $\Gamma^{\sigma\pi}$ above $x \simeq 0.10$ might arise from short-range order in the single crystal structures [9], or from local inhomogeneities in the C content on a microscopic scale [21].

Finally, these results give an indication of what an ideal substitution, capable of increasing the T_c of the MgB_2 system, should do, i.e. increase $\lambda_{\sigma\sigma}$, decrease $\mu_{\sigma\sigma}^*$, and keep the interband scattering as small as in pure MgB_2 . According to eqs. 3 and 5, this is possible if $N_N^\sigma(E_F)$ increases and $N_N^\pi(E_F)$ decreases.

Many thanks are due to S. Massidda and A. Bianconi for useful discussions. This work was done within the Project PRA UMBRA of INFM, the FIRB Project RBAU01FZ2P and the INTAS Project n.01-0617.

[1] J. Nagamatsu, N. Nakagawa, T. Muranaka, Y. Zenitani and J. Akimitsu, *Nature (London)* 410, 63 (2001).
[2] Y. Kong, O.V. Dolgov, O. Jepsen, O.K. Andersen, *Phys. Rev. B* 64, 020501 (2001); J. Kortus et al., *Phys. Rev. Lett.* 86, 4656 (2001); S. Shulga et al., *cond-mat/0103154*; J.M. An and W. Pickett, *Phys. Rev. Lett.* 86, 4366 (2001).
[3] A.Y. Liu, I.I. Mazin and J. Kortus, *Phys. Rev. Lett.* 87, (2001) 087005;
[4] A. Brinkman, A.A. Golubov, H. Rogalla, O.V. Dolgov, J. Kortus, Y. Kong, O. Jepsen, O.K. Andersen, *Phys. Rev.*

B 65, 180517(R) (2002); A.A. Golubov, A. Brinkman, O.V. Dolgov, J. Kortus, O. Jepsen, *Phys. Rev. B* 66, 054524 (2002).
[5] H.J. Choi, D. Roundy, H. Sun, M.L. Cohen and S.G. Louie, *Nature (London)* 418, 758 (2002).
[6] R.J. Cava, H.W. Zandbergen and K. Inumaru, *Physica C* 385, 8 (2003).
[7] Z. Holánová, P. Szabó, P. Samuely, R.H.T. Wilke, S.L. Bud'ko, P.C. Canfield, *Phys. Rev. B* 70, 064520 (2004).
[8] R.S. Gonnelli, D. Daghero, A. Calzolari, G.A. Ummarino, Valeria Dellarocca, V.A. Stepanov, J. Jun, S.M. Kazarov

- and J. Karpinsky, preprint cond-mat/0407265.
- [9] A.H. Moudden, Submitted to J.Phys. Chem. Solids.
- [10] A.A. Golubov, J. Kortus, O.V. Dolgov, O. Jepsen, Y. Kong, O.K. Andersen, B.J. Gibson, K. Ahn, and R.K. Kremer, J. Phys.: Condens. Matter 14, 1353 (2002).
- [11] G.M. Eliashberg, Sov. Phys. JETP 3, 696 (1963); D.J. Scalapino, in "Superconductivity" edited by R.D. Parks (Marcel Dekker Inc, N. Y.) 449 (1969); J.P. Carbotte, Rev. Mod. Phys. 62, 1028 (1990); P.B. Allen and B. Mitrovich, "Theory of superconducting T_c ", in Solid State Physics, Vol. 37, edited by H. Ehrenreich F. Seitz, D. Turnbull, (Academic Press, New York, 1982); F. Marsiglio and J.P. Carbotte, "The Physics of Conventional and Unconventional Superconductors", edited by K.H. Bennemann and J.B. Ketterson (Springer-Verlag).
- [12] F. Marsiglio, Jour. of Low Temp. Phys. 87, 659 (1992).
- [13] S.V. Shulga, S.L. Drechsler, G. Fuchs, K.H. Muller, K. Winzer, M. Heinecke and K. Krug, Phys. Rev. Lett. 80, 1730 (1998); S.D. Adrian, S.A. Wolf, O.V. Dolgov, S. Shulga, V.Z. Kresin, Phys. Rev. B 56, 7878 (1997).
- [14] G.A. Ummarino, R.S. Gonnelli, S. Massidda and A. Bianconi, Physica C 407, 121 (2004).
- [15] I.I. Mazin, V.P. Antropov, Physica C 385, 49 (2003).
- [16] O.V. Dolgov, R.S. Gonnelli, G.A. Ummarino, A.A. Golubov, S.V. Shulga and J. Kortus, Phys. Rev. B 68, 132503 (2003).
- [17] G. Grimvall, The electron-phonon interaction in metals, (North Holland, Amsterdam, 1981).
- [18] G. Profeta, A. Continenza and S. Massidda, Phys. Rev. B 68, 144508 (2003).
- [19] O.V. Dolgov, talk at the 6th European Conference on Applied Superconductivity (EUCAS), Sorrento, Italy, September 14-18, 2003; I. I. Mazin, O. K. Andersen, O. Jepsen, A. A. Golubov O.V. Dolgov and J. Kortus, Phys. Rev. B 69, 056501 (2004).
- [20] I. I. Mazin, O. K. Andersen, O. Jepsen, O.V. Dolgov, J. Kortus, A. A. Golubov, A. B. Kuzmenko, and D. van der Marel, Phys. Rev. Lett. 89, 107002 (2002).
- [21] S.M. Kazakov, R. Puzniak, K. Rogacki, A.V. Mironov, N.D. Zhigadlo, J. Jun, Ch. Soltmann, B. Batlogg and J. Karpinski, preprint cond-mat/0405060.
- [22] J. Kortus, O.V. Dolgov, R.H. Kremer, and A.A. Golubov, cond-mat/0411667.
- [23] S.C. Erwin and I.I. Mazin, Phys. Rev. B 68, 132505 (2003).
- [24] E. Cappelluti, S. Ciuchi, C. Grimaldi, L. Pietronero, S. Strässler, Phys. Rev. Lett. 88, 117003 (2002).
- [25] P. Morel and P. W. Anderson, Phys. Rev. 125, 1263 (1962); G.A. Ummarino, R.S. Gonnelli, Phys. Rev. B 66, 104514 (2002).
- [26] R.J. Soulen, Jr., M.S. Osofsky, L.D. Cooley, Phys. Rev. B 68, 094505 (2003).
- [27] H. Suhl, B.T. Matthias, and L.R. Walker, Phys. Rev. Lett. 3, 552 (1959).